ACS APPLIED MATERIALS & INTERFACES

Research Article

Cite This: ACS Appl. Mater. Interfaces 2019, 11, 24298−24307

www.acsami.org

Gas Sensor by Direct Growth and Functionalization of Metal Oxide/Metal Sulfide Core−Shell Nanowires on Flexible Substrates

Daejong Yang,[†] Incheol Cho,[‡] Donghwan Kim,[§] Mi Ae Lim,[‡] Zhiyong Li,[∥] Jong G. Ok,[⊥] Moonjin Lee,[#] and Inkyu Park*[,‡,¶]

[†]Department of Mechanical and Automotive Engineering, Kongju National University, 1223-24 Cheonan-daero, Seobuk-gu, Cheonan, Chungcheongnam-do 31080, South Korea

[‡]Department of Mechanical Engineering and [¶]KI for the NanoCentury, Korea Advanced Institute of Science and Technology (KAIST), 291 Daehak-ro, Yuseong-gu, Daejeon 34141, South Korea

[§]Korea Electric Power Research Institute (KEPRI), Korea Electric Power Corporation (KEPCO), 105 Munji-ro, Yuseong-gu, Daejeon 34056, South Korea

[∥]Systems Research Lab, Hewlett Packard Laboratory, 1501 Page Mill Rd, Palo Alto, California 94304, United States

[⊥]Department of Mechanical and Automotive Engineering, Seoul National University of Science and Technology, 232 Gongneung-ro, Nowon-gu, Seoul 01811, South Korea

[#]Korea Research Institute of Ships & Ocean Engineering, 1312-32 Yuseong-daero, Yuseong-gu, Daejeon 34103, South Korea

Supporting Information

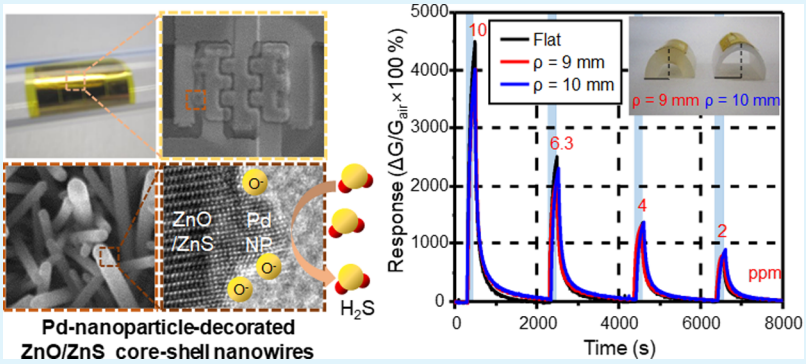

ABSTRACT: We have developed a novel fabrication method for flexible gas sensors for toxic gases based on sequential wet chemical reaction. In specific, zinc oxide (ZnO) nanowires were locally synthesized and directly integrated on a flexible polymer substrate using localized hydrothermal synthesis methods and their surfaces were selectively functionalized with palladium (Pd) nanoparticles using a liquid phase deposition process. Because the entire process is conducted at a low temperature in a mild precursor solution, it can be applied for flexible substrates. Furthermore, the surface of ZnO nanowires was sulfurized by hydrogen sulfide (H_2S) gas to form zinc oxide/zinc sulfide (ZnO/ZnS) core−shell nanowires for stable sensing of H_2S gas. The locally synthesized ZnO/ZnS core−shell nanowires enable an ultracompact-sized device, and Pd nanoparticles improve the sensing performance and reduce the operating temperature (200 °C). The device shows a high sensitivity [$(G_{gas} - G_{air})/G_{air} \times 100\%$ = 4491% to 10 ppm], fast response (response/recovery time <100 s) to hydrogen sulfide, and outstanding selectivity (>100 times) to other toxic gases (e.g., carbon monoxide, acetone, ethanol, and toluene). Moreover, vertically synthesized nanowires provide a long bending path, which reduces the mechanical stresses on the structure. The devices showed stable gas sensing performance under 9 mm positive radius of curvature and 5 mm negative radius of curvature. The mechanical robustness of the device was also verified by numerical simulations which showed dramatic decrease of maximum stress and strain to 4.2 and 5.0%, respectively.

KEYWORDS: *local synthesis, surface functionalization, flexible sensor, gas sensor, semiconductor nanowire*

INTRODUCTION

As the market for the wearable electronic devices rapidly grows, there have been technological advances on wearable and flexible physical/chemical sensors. Especially, flexible gas sensors detecting toxic gases (NO_x, CO, H_2S, VOCs, etc.) or bio-markers (acetone, NH_3, CH_4S, etc.) from human breathing have great potential to improve the quality of human life. Materials such as graphene, conductive polymers, carbon

Received: April 21, 2019
Accepted: June 12, 2019
Published: June 12, 2019

DOI: 10.1021/acsami.9b06951
ACS Appl. Mater. Interfaces 2019, 11, 24298−24307

nanotubes, and so forth have been widely used as sensing materials for flexible gas sensors because of their high sensitivity, mechanical robustness, optical transparency, and low working temperature (i.e., room temperature).[1−8] However, they suffer from slow response and incomplete recovery to the initial state after a sensing event. Furthermore, their sensing performances can be easily affected by mechanical deformation.[2,3,6] Therefore, these sensors are not capable of producing repeatable sensing signals at room temperature under mechanical deformation.[6,9]

As another candidate sensing material, one-dimensional (1D) metal oxide nanomaterials including nanowires, nanotubes, nanorods, and nanofibers have shown great promises in high-performance gas sensors with high sensitivity, low detection limit (sub-ppm or ppb levels), and fast response (90% response time less than a few seconds). 1D nanomaterials are not only able to be integrated into a small area but also have a high surface-to-volume ratio, which provides large reaction area. Because of these advantages, they can be easily combined with integrated circuit devices and show excellent gas sensing performance.[10−18] In addition, the nanowires combined with metal nanoparticles promote the reaction between target gas and sensing material because of their unique physical and chemical properties.[19−26] 1D metal oxide nanomaterial-based gas sensors were usually fabricated by the chemical synthesis of nanomaterials, followed by their subsequent assembly on prefabricated electrodes via jet printing, drop casting, and screen printing[27−29] or by the fabrication of electrodes on the pre-deposited film of nanomaterials.[30,31] Although these methods are simple, it is very difficult to downscale the size of nanomaterial networks toward highly integrated and ultracompact devices with low power consumption for the high-temperature heating of sensing materials. Furthermore, the robust contact between flexible substrate, electrodes, and integrated nanomaterials cannot be guaranteed by the above-mentioned methods because the bonding is based on the weak van der Waals force or electrostatic force. The brittleness of metal oxide nanomaterials can also be a barrier to their applications in flexible sensors with large deformation.

In order to overcome these technical issues, many researchers studied to directly synthesize nanomaterials on the flexible substrate;[32−35] we have developed a facile method to directly grow 1D metal oxide nanomaterials in a microscale area on a flexible substrate by localized temperature control.[36] First, a microheater and electrodes were fabricated on a flexible, high-temperature-resistant polyimide (PI) substrate. The microheater generates a thermal energy field through local heating in the liquid precursor, resulting in the selective synthesis of zinc oxide (ZnO) nanowires via hydrothermal reaction. ZnO nanowires grown between electrodes formulate networks through contact with each other, so that an electrical path can be created. The microheater used for the nanowire synthesis is also used to maintain an elevated temperature of sensing nanomaterials during the gas sensor operation. Moreover, we have developed a localized surface functionalization process to enhance the gas sensing performance of the locally synthesized ZnO nanowires. In order to uniformly decorate the surface of ZnO nanowires with palladium (Pd) nanoparticles, we also used hydrothermal deposition of Pd through the local thermal energy generated by the microheater. Furthermore, the surface of sensing materials was sulfurized to form a zinc sulfide (ZnS) layer for stable hydrogen sulfide (H_2S) sensing. The gas sensing performances (e.g., sensitivity, response speed, and selectivity against other gases) of ZnO/ZnS core−shell nanowires were greatly improved by the catalytic effect of Pd nanoparticles. Because the synthesis process requires a low temperature below the boiling point of water and mild liquid precursor solutions, it can be applied for eco-friendly and low-cost fabrication on flexible substrates. In addition, this direct synthesis method achieves mechanical robustness of the devices. It allowed for strong bonding between nanostructures and substrate, and vertically oriented nanostructures reduced stress by providing the long bending path. These facts were theoretically and experimentally analyzed by numerical simulation and experimental studies such as tensile and bending tests.

MATERIALS AND METHODS

Fabrication of a Flexible Microheater Device. The liquid PI varnish (POLYZEN 150P, PICOMAX, South Korea) was spin-coated on a clean Si substrate to make a 35 μm thick PI film. It was then cured in a convection oven by increasing the temperature from room temperature to 300 °C for 2 h to form a solid film, which was used as a base substrate for the flexible sensor device. A photoresist (PR; AZ5214, MicroChemicals GmbH, Germany) was patterned on the substrate by photolithography, and Ti (10 nm) and Pt (200 nm) layers were deposited and patterned on the substrate by the e-beam evaporation and lift-off process. Then, the liquid PI varnish was spin-coated again on the substrate and cured to form a 1 μm thick PI layer for the electrical insulation between the heater and sensing electrodes. PR (AZ5214) was patterned again on the PI layer for interdigitated electrodes by aligning with underlying microheaters. Cr (10 nm) and Au (200 nm) layers were deposited on the substrate, and PR layer and dummy Au film were lifted-off in acetone. PR (AZ9260, MicroChemicals GmbH, Germany) was spin-coated and patterned to open contact pads for the microheater, and the second PI layer on the contact pads for the microheater was developed in the PI developer (PI developer, picoMAX, South Korea). Finally, the edge of the PI film was slightly torn off and pulled apart to detach the film from the Si handling wafer. The same Si handling wafer was reused for the fabrication of additional devices.

Synthesis of Pd-Coated ZnO Nanowires and ZnO/ZnS Core−Shell Nanowires. The prefabricated substrate was coated with a ZnO-textured seed solution [5 mM zinc acetate dehydrate ($Zn(O_2CCH_3)_2{\cdot}(H_2O)_2$) in ethanol] and then heated at 350 °C for 20 min on a hotplate.[37] Zinc nitrate hexahydrate ($Zn(NO_3)_2{\cdot}6H_2O$; 25 mM), hexamethylenetetramine ($C_6H_{12}N_4$; 25 mM), and polyethyleneimine ($(C_2H_5N)_n$; 6 mM) were mixed in deionized (DI) water for the ZnO nanowire precursor solution.[36−40] Sodium citrate dihydrate ($C_6H_5Na_3O_7{\cdot}2H_2O$; 30 mM) and potassium chloropalladite (K_2PdCl_4; 1 mM) were dissolved in DI water, and pH of the solution was adjusted to 11 by adding 0.1 M sodium hydroxide (NaOH) aqueous solution.[41−43] (All chemicals were purchased from Sigma-Aldrich.) A PDMS block with a punched hole (diameter = 5 mm) was attached on the microheater device, and 10 μL of ZnO nanowire precursor solution was supplied. A dc bias of 0.42 V and a power of 67 mW were applied to the microheater for 12−15 min for Joule heating. After the synthesis of ZnO nanowires and rinsing with DI water, the PDMS block was replaced and 10 μL of the Pd nanoparticle precursor solution was supplied. A dc bias of 0.38 V and power of 44 mW were applied to the microheater for 6 min. Afterward, the device was rinsed with DI water and blow dried with N_2 gas. The devices were exposed to 20 ppm H_2S gas for 20 min to form a ZnS layer for stable gas sensing.

Characterization of Synthesized Materials. The physical and chemical characteristics of the devices for each fabrication step and before and after the H_2S exposure were analyzed using field emission scanning electron microscopy (SEM, Sirion, FEI, USA) and field emission transmission electron microscopy (TEM, Tecnai G^2 F30 super twin, FEI, USA). The X-ray photoelectron spectroscopy (XPS,

DOI: 10.1021/acsami.9b06951
ACS Appl. Mater. Interfaces 2019, 11, 24298−24307

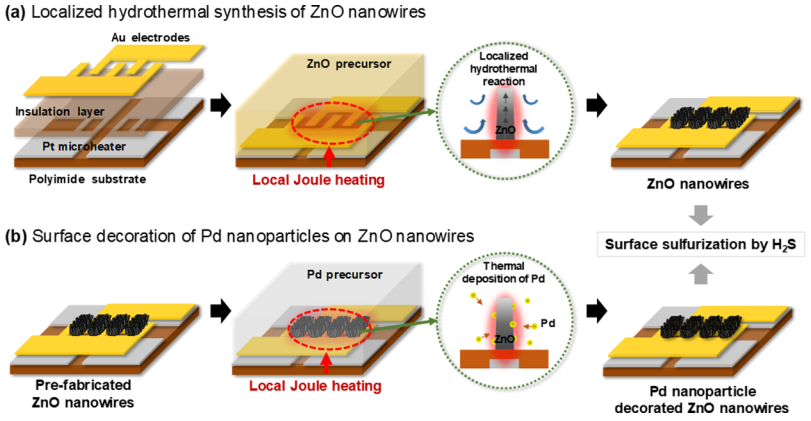

Figure 1. Schematic illustrations of (a) pristine zinc oxide (ZnO) nanowire synthesis process on a PI substrate via local heating and (b) palladium (Pd) nanoparticle coating process on the surface of ZnO nanowires via local heating.

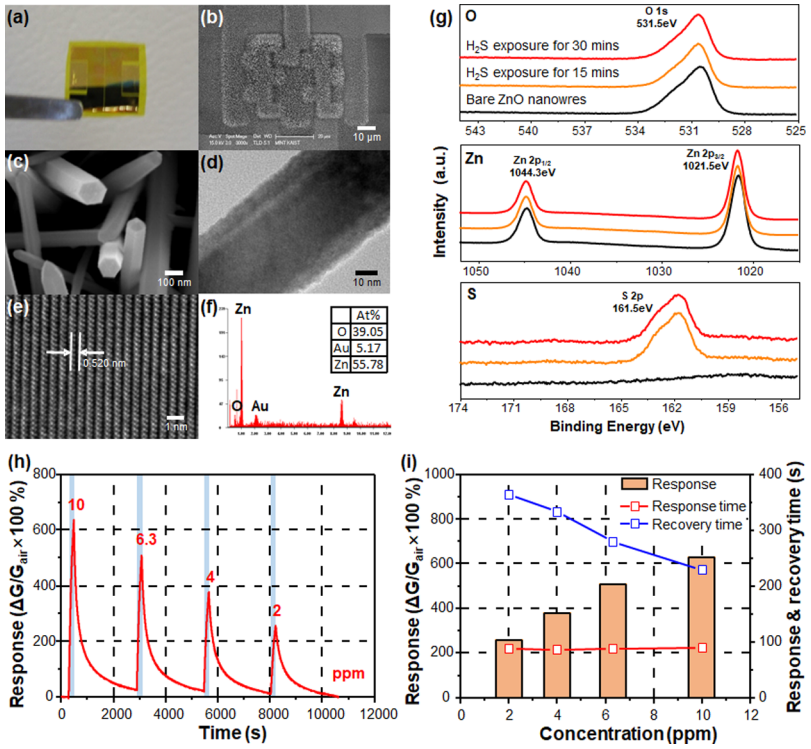

Figure 2. Fabrication results of zinc oxide (ZnO) nanowire sensor on a flexible substrate and hydrogen sulfide (H_2S) gas sensing result. (a) Photograph of the flexible sensor. (b,c) SEM images, (d,e) TEM images and (f) EDS data of locally synthesized ZnO nanowire device. (g) XPS data of ZnO nanowires and zinc oxide/zinc sulfide (ZnO/ZnS) core−shell nanowires sulfurized for 15 and 30 min. (h) Dynamic gas sensing response and (i) relationship of response-gas concentration, response, and recovery time of ZnO/ZnS core−shell nanowires under H_2S gas.

K-Alpha+, Thermo Fisher Scientific, USA) spectra of bare ZnO nanowires and ZnO/ZnS core−shell nanowires sulfurized for 15 and 30 min were measured.

H_2S Gas Sensing. The devices were mounted in a gas sensing chamber and connected to a power supply (E3642A, Agilent, USA) and a source meter (2400, Keithley, USA) for Joule heating and resistance measurement, respectively. H_2S gas (500 sccm) was supplied to the sensor device, and the concentration of H_2S gas was adjusted by controlling the flow rates of air-balanced 20 ppm H_2S gas and dry air (0% relative humidity) with mass flow controllers. A 0.65 V dc bias was applied to the microheater to heat the sensing materials to operating temperature, and 0.1 V dc bias was applied to the sensing materials to measure their resistance. Gas tests were conducted under 2−10 ppm H_2S gas. In order to characterize the gas sensing performance under bending condition, the sensors were mounted on the inside and outside surfaces of a silicone tube with various diameters. The gas tests were conducted under 9 and 10 mm positive radii of curvature and under 5 and 8 mm negative radii of curvature.

Numerical Simulation of Nanomaterial Behavior under Mechanical Deformation. The numerical simulation of nanomaterials under bending conditions was conducted using a finite element method simulator (COMSOL Multiphysics 5.2, COMSOL, Inc., USA) with a solid mechanics model (steady state linear elasticity, $\nabla\cdot\boldsymbol{\sigma} + \mathbf{F} = \mathbf{0}$). The geometries of nanowires were constructed with different lengths, a fixed width, and horizontally/vertically aligned directions (length = 2 and 5 μm, width = 100 nm, tilting angle of vertically aligned nanowires = 87°). Two percent tensile and compressive strains were applied on the nanowires to describe the mechanical bending of the substrate, and the stress and strain distributions were calculated.

Tensile Test. The sensor device was mounted on the laboratory-made tensile loading setup. The device was stretched by ε = 1.2, 2.4,

DOI: 10.1021/acsami.9b06951
ACS Appl. Mater. Interfaces 2019, 11, 24298−24307

5.5, and 7.5% tensile strains and released to zero tensile force. The device mounted on the tensile loading setup was observed by using SEM for each tensile loading and recovery step.

RESULTS AND DISCUSSION

For localized heating to induce selective synthesis of ZnO nanowires, microheater-embedded devices were fabricated using a conventional microelectro-mechanical-system microfabrication process. As shown in Figure S1, the device consisting of a microheater and sensing electrodes was fabricated on the PI film. The ZnO nanowire precursor solution was supplied, and a dc bias voltage was applied to the microheater to generate a local hot spot via Joule heating. The temperature of the microheater was adjusted around 95 °C by supplying 5−10% less electrical power than that for the precursor solution to reach the boiling point of water (100 °C). The precursor solution adjacent to the microheater was locally heated, and ZnO nanowires were selectively synthesized by the local endothermic reaction (Figure 1a).

Figure 2a−c shows a photo and SEM image of ZnO nanowires, whose average diameter and length are around 100 nm and 5 μm, respectively. The nanowires were synthesized from each microheater and formed a bridging structure between the interdigitated sensing electrodes. Figure 2d−f shows a TEM image and energy-dispersive X-ray spectroscopy (EDS) spectrum of synthesized ZnO nanowires. A lattice spacing of 0.52 nm shown in Figure 2e well corresponds to the *d*-spacing (001) of ZnO nanowires,[44] and the EDS data also verified that ZnO nanowires were successfully synthesized.

As mentioned above, the ZnO nanowire is a widely used material for gas sensors because of its large surface-to-volume ratio and unique electron transport properties.[45−48] Moreover, the network structure synthesized in this work provides a large surface-to-volume ratio and numerous nanowire−nanowire junctions and metal−nanowire junctions that facilitate a high sensitivity. Under ambient condition, oxygen molecules are adsorbed on the surface of ZnO nanowires and take electrons from ZnO nanowires, enlarging the electron depletion region and increasing the electrical resistance. When exposed to hydrogen sulfide (H_2S) gas, its molecules react with adsorbed oxygen molecules and donate the electrons and detach oxygen molecules from ZnO nanowires. As a consequence, the resistance of ZnO nanowires is decreased.[49] In order to enhance the gas sensing response and to reduce the influence of humidity, the sensor should be heated at high temperature.[50] In our device, the microheater used for the ZnO nanowire synthesis can also be used to maintain high temperature during the gas sensor operation. A dc bias of 0.65 V was applied to the microheater during the sensor operation, and the temperature was estimated to be around 200 °C by measuring the resistance change of the Pt microheater (Figure S2). However, pristine ZnO is not suitable for the H_2S sensor because ZnO reacts with H_2S gas and transforms to ZnS. H_2S is decomposed to HS^- and S^{2-} sequentially, and then S^{2-} is combined with ZnO by the following reaction[51]

$$ZnO(s) + H_2S(ads) \rightarrow ZnS(s) + H_2O(g) \quad (1)$$

This reaction is irreversible at low temperature because the enthalpy change is negative. In order to avoid this unstable sensing condition, ZnO nanowires were exposed to 20 ppm H_2S gas at 200 °C for 20 min. Because the devices have been exposed to high temperature and high concentration of H_2S conditions for a long time, stable ZnO/ZnS core−shell nanostructures are formed. Thus, the sensors keep stable composition under low concentration of H_2S gas under 10 ppm, which is the 8 h exposure limit for workers by Occupational Safety and Health Administration (Standards—29 CFR).[52]

Figure S3 shows high-resolution TEM (HRTEM) images of ZnO nanowires and ZnO/ZnS core−shell nanowires sulfurized for 15 and 30 min by exposure to H_2S gas. ZnO nanowires show clear edges (Figure S3a), whereas sulfurized ZnO/ZnS core−shell nanowires show boundaries between ZnO and ZnS (Figure S3b,c). The spaces between adjacent lattice planes are 0.253 nm at the surface of ZnS and 0.262 nm at the core of ZnO (Figure S3b). They correspond to (002) and (108) planes of the wurtzite structure of ZnO and ZnS, respectively.[53] The thicknesses of surface ZnS are both ∼10 nm for the samples sulfurized for 15 and 30 min. This reflects that the sulfurization reached an equilibrium state after 15 min of H_2S exposure. Figure 2g shows the result of XPS of ZnO nanowires (black line) and ZnO/ZnS core−shell nanowires sulfurized for 15 (orange line) and 30 min (red line). The sulfur peaks of ZnO/ZnS core−shell nanowires are clearly observed in the XPS results. The sulfur peak intensities of ZnO/ZnS core−shell nanowires sulfurized for 15 and 30 min were quite similar. This result shows that the amounts of sulfur in two samples are similar and correspond to the same ZnS thickness as shown in the TEM images (Figure S3). These results verify that 15 min is long enough to form chemically stable ZnO/ZnS core−shell nanowires.

ZnS can be made as an n-type or p-type semiconductor depending on its defects,[54] but in this work, it shows n-type characteristics because it has a core−shell structure with ZnO.[55,56] Therefore, its H_2S sensing mechanism is basically the same as that for ZnO, and the additional electronic transfer process from ZnS to ZnO is added.[56] Because the conduction band of ZnS is located at higher potential than that of ZnO, electrons transfer from the conduction band of ZnS to the conduction band of ZnO until their Fermi levels equalize.[56,57] This electron transfer generates an additional electron depletion layer at the ZnO/ZnS interface. H_2S molecules react with adsorbed oxygen molecules on the surface of ZnS, and they were transformed to H_2O and SO_2 molecules. During this reaction, electrons are released from the oxygen ions and transferred to the depletion layer on the surface of ZnS and at the ZnO/ZnS interface.[56]

$$H_2S_{(g)} + 3O_{(ads)}^- \rightarrow H_2O_{(g)} + SO_{2(g)} + 3e^- \quad (2)$$

In order to identify the sensing characteristics such as sensitivity, response time, and recovery time, 10, 6.3, 4, and 2 ppm of H_2S gas were supplied to the ZnO/ZnS core−shell nanowire device for 250 s, followed by refreshing with a dry air for 2500 s. As shown in Figure 2h, the conductance of the ZnO/ZnS core−shell nanowire sensor was increased and the responses $[S = (G_{gas} - G_{air})/G_{air} \times 100\%]$ were calculated as 631, 507, 377, and 256% to 10, 6.3, 4, and 2 ppm of H_2S gas for 250 s, respectively, where G_{gas} and G_{air} are the conductances of the sensor in the H_2S gas and air, respectively. The response and recovery times (from 10 to 90% of maximum sensor response at 250 s of H_2S exposure) were 90, 88, 85, and 87 s and 229, 279, 333, and 364 s to 10, 6.3, 4, and 2 ppm of H_2S gas, respectively (Figure 2i).

Even though the shape and size of the synthesized ZnO nanowire bundles were quite uniform in the same synthesis

DOI: 10.1021/acsami.9b06951
ACS Appl. Mater. Interfaces 2019, 11, 24298−24307

condition, the shape of the individual nanowire and connection forms were different. In order to make more uniform device, 0.01 V dc bias was applied to the sensing electrodes and the current through nanowires was measured during the synthesis process (see Figure S4a in the Supporting Information). The sensitivity is related to the junction of nanowires, and it can be monitored by measuring the resistance of the nanowire bundle. As shown in Figure S4b, the current through the ZnO nanowire bundle was increased by increasing the synthesis time. When the current reaches a certain value (0.2 μA), the power supply was stopped. Figure S4c shows that the gas sensing responses of three different sensors fabricated by this procedure were quite uniform under 10 ppm H_2S gas.

In order to improve the gas sensing performance of ZnO nanowires, Pd nanoparticles were coated on the surface of ZnO nanowires. This reaction is also activated by local heating, and the same setup for the local hydrothermal reaction was utilized except for the precursor solution (Figure 1b). The temperature of the microheater was locally elevated to ~95 °C, and the heat was efficiently propagated along ZnO nanowires because of its thermal conductivity [6.5 W/(m·K) at 100 °C][58] that is 36 times higher than that of the substrate material [PI, 0.18 W/(m·K) at 300 K].[59] The increased temperature accelerated the reduction of the metal salt ions, and Pd nanoparticles were synthesized on the surface of ZnO nanowires. Figure 3a–d shows the SEM and TEM images of

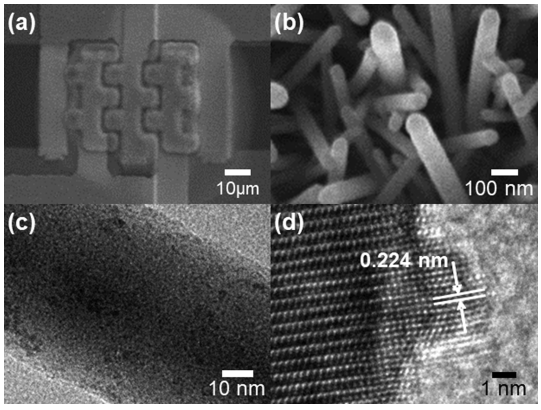

Figure 3. Fabrication results of palladium (Pd) nanoparticles synthesized on zinc oxide (ZnO) nanowires. (a,b) SEM images and (c,d) TEM images of locally synthesized Pd nanoparticle-coated ZnO nanowires.

Pd nanoparticle-decorated ZnO nanowires. Pd nanoparticles with an average diameter of 3 nm were uniformly coated, whereas the shapes of ZnO nanowires were not changed during the coating process of Pd nanoparticles. A space of 0.224 nm between adjacent lattice planes in the HRTEM image (Figure 3d) is well matched to the (111) planes of the face-centered cubic phase of Pd.[60] EDS data in Figure S5 also show that Pd elements are present on the surface of ZnO nanowires. Therefore, we can conclude that Pd nanoparticles were successfully synthesized.

The gas sensing performance of semiconductor materials can be greatly improved by coating with noble metal nanoparticles. The Pd nanoparticles act as a catalyst for the dissociation of H_2S molecules by the spill-over effect.[26,61−63] They release electrons quickly from H_2S to the surface of ZnO/ZnS core−shell nanowires and increase the quantity of reacted H_2S molecules. This improves the reaction between gas molecules and sensing materials. As mentioned above, for a stable H_2S gas sensing, Pd nanoparticle-decorated ZnO nanowires were also exposed to 20 ppm of H_2S gas at 200 °C for 20 min in order to form ZnO/ZnS core−shell nanowires.

The Pd nanoparticle-decorated ZnO/ZnS core−shell nanowires were exposed to 10, 6.3, 4, and 2 ppm of H_2S gas, whereas 0.65 V dc bias was applied to the microheater. As shown in Figure 4a, the response of Pd-decorated ZnO/ZnS

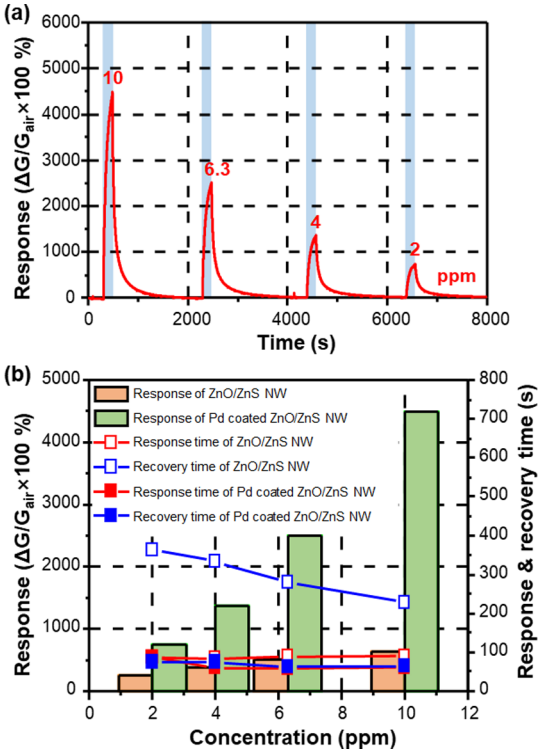

Figure 4. Hydrogen sulfide (H_2S) gas sensing result of palladium (Pd) nanoparticle-decorated zinc oxide/zinc sulfide (ZnO/ZnS) core−shell nanowire device. (a) Response vs time graph of Pd nanoparticle-decorated ZnO/ZnS core−shell nanowires and (b) comparison of response, response time, and recovery time vs H_2S concentration between ZnO/ZnS core−shell nanowires and Pd nanoparticle-decorated ZnO/ZnS core−shell nanowires.

core−shell nanowires was 4491, 2506, 1379, and 750% under 10, 6.3, 4, and 2 ppm of H_2S gas, respectively. The response−concentration graphs of ZnO/ZnS core−shell nanowires with and without Pd coating indicate that the Pd nanoparticles dramatically enhanced the sensitivity of the ZnO/ZnS core−shell nanowire sensor (Figure 4b). Moreover, the response times of Pd-decorated ZnO/ZnS core−shell nanowires (86 s at 2 ppm; 60 s at 4 ppm; 58 s at 6 ppm; and 61 s at 10 ppm) were shorter than those of bare ZnO/ZnS core−shell nanowires (87 s at 2 ppm; 85 s at 4 ppm; 88 s at 6 ppm; and 90 s at 10 ppm). More importantly, the recovery times of Pd-decorated ZnO/ZnS core−shell nanowires (76 s at 2 ppm; 76 s at 4 ppm; 63 s at 6 ppm; and 62 s at 10 ppm) were dramatically reduced compared to those of bare ZnO/ZnS core−shell nanowires (364 s at 2 ppm; 333 s at 4 ppm; 279 s at 6 ppm; and 229 s at 10 ppm). These enhancements are due to the surface catalytic effect of Pd nanoparticles. The Pd nanoparticles reduce the activation energy for the adsorption and desorption; therefore, the surface reaction coefficient is increased.[64] As a result, the

DOI: 10.1021/acsami.9b06951
ACS Appl. Mater. Interfaces 2019, 11, 24298−24307

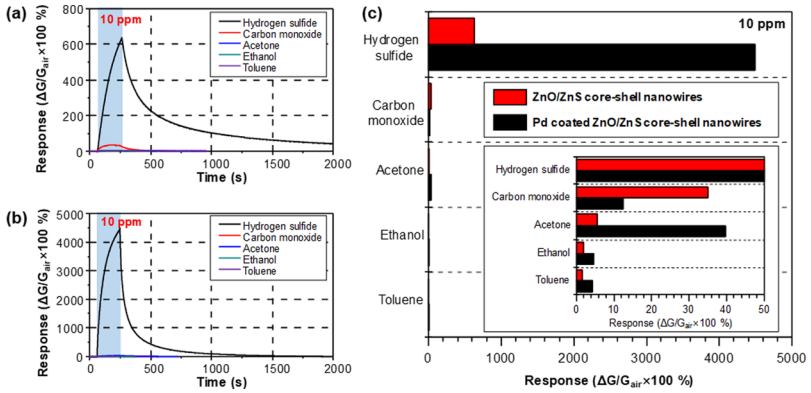

Figure 5. Gas sensing characteristics of (a) zinc oxide/zinc sulfide (ZnO/ZnS) core–shell nanowire sensor and (b) palladium (Pd) nanoparticle-decorated ZnO/ZnS core–shell nanowire sensor to 10 ppm hydrogen sulfide, carbon monoxide, acetone, ethanol, and toluene. (c) Summary of responses to various toxic gases.

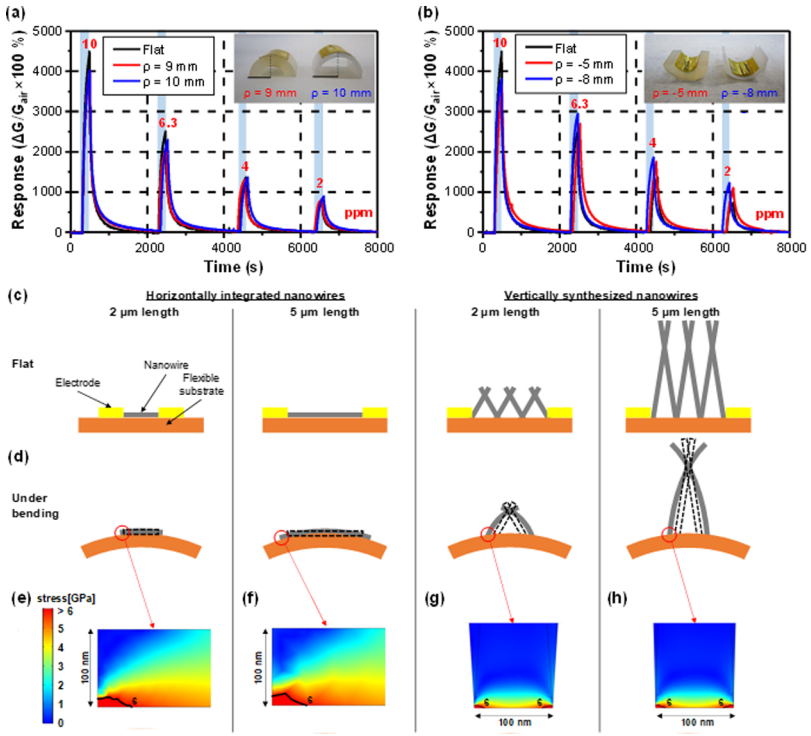

Figure 6. Hydrogen sulfide (H_2S) gas sensing performance of palladium (Pd) nanoparticle-decorated zinc oxide/zinc sulfide (ZnO/ZnS) core–shell nanowires under bending conditions. Comparison of the sensing performances between (a) flat and positively bent surfaces (curvature radii: 9 and 10 mm) and (b) flat and negatively bent surfaces (curvature radii: −5 and −8 mm); schematic illustrations of deformation of horizontally integrated and vertically synthesized ZnO nanowires (c) in flat and (d) under the same bending conditions; stress profile at the edge of the horizontally integrated nanowire with (e) 2 and (f) 5 μm length and vertically synthesized nanowire with (g) 2 and (h) 5 μm length under 2% tensile loading.

Pd-decorated ZnO/ZnS core–shell nanowire sensor shows fast response and recovery.

Figure 5a,b shows the response of ZnO/ZnS core–shell nanowires and Pd-decorated ZnO/ZnS core–shell nanowires to 10 ppm of several reducing gases [i.e., H_2S, carbon monoxide (CO), acetone (C_3H_6O), ethanol (C_2H_5OH), and toluene ($C_6H_5CH_3$)]. In the case of the ZnO/ZnS core–shell nanowire sensor, the response to 10 ppm H_2S (631%) was higher than those to the same concentration of carbon monoxide (35%), acetone (5.7%), ethanol (2%), and toluene (1.53%) (Figure 5c). The selectivity for target gas can be summarized as the ratio between the response to the target gas (H_2S) and the response to the other gases (18, 110.7, 315.5, and 412.4 against CO, acetone, ethanol, and toluene, respectively). The responses of Pd-decorated ZnO/ZnS core–shell nanowires show enhanced sensing performance for almost all gas species (4444% for H_2S, 12.37% for CO, 39.68% for acetone, 4.7% for ethanol, 4.3% for toluene, and 10 ppm for all gases). However, the selectivity to H_2S against other gases became much better for all gas species (359.3 for CO, 112 for acetone, 945.5 for ethanol, and 1033.5 for toluene). These results show that the Pd nanoparticles contribute not only to the enhancement of sensitivity but also to the dramatic improvement of the selectivity for H_2S. Metal oxide-based flexible H_2S sensors have been rarely researched; thus, this work provides novel methods for

DOI: 10.1021/acsami.9b06951
ACS Appl. Mater. Interfaces 2019, 11, 24298–24307

developing flexible H_2S gas sensors. As summarized in Table S2 in the Supporting Information, our sensors show good performances as compared to those of the state-of-the-art flexible gas sensors.

As explained above, we have integrated Pd nanoparticle-decorated ZnO/ZnS core−shell nanowire sensors on the PI film and confirmed an outstanding H_2S gas sensing performance. Moreover, mechanical reliability of the sensor device is crucially important for practical applications such as wearable devices. Therefore, it is essential to confirm a stable sensing response under mechanical stresses. The most common mechanical loading for flexible devices is bending. In order to characterize the mechanical reliability under bending condition, the sensor was attached on curved surfaces, positively bent with curvature radii of 9 and 10 mm and negatively bent with curvature radii of 5.0 and 8.0 mm. The responses of bent sensors to 2−10 ppm of H_2S gas were measured, and no significant difference of response was observed between flat, positively bent, and negatively bent conditions (Figure 6a,b). This is because the direct synthesis of ZnO nanowires on the substrate via localized Joule heating of the microheater provided strong bonding between substrate and nanowires. Figure 6c,d shows schematic illustrations of deformation of horizontally integrated and vertically synthesized ZnO nanowires under the same bending conditions. Vertically synthesized ZnO nanowires provide long bending path, which reduces the mechanical stresses on the structure. In order to verify it, we have conducted a numerical simulation of deformation and stress in horizontally integrated nanowire and vertically synthesized nanowire with lengths of 2 and 5 μm under 2% tensile and compressive strain conditions using COMSOL Multiphysics. Figures S6 and S7 show the stress profiles of these four structures under tensile and compressive stresses, respectively. In all of these four cases, the large stresses were observed at the edge of the nanowires (see vertex at 2-dimensional figures in Figure S6 and Table S1a). In the magnified image of stress at the edge (Figure 6e−h), black lines indicate the location where the fracture occurs [stress > ultimate strength of ZnO nanowire (6 GPa)].[65] The fracture occurs on the relatively large area at the horizontally integrated nanowires (Figure 6e,f), whereas the fracture occurs on the tiny portion of the edge at the vertically synthesized nanowires (Figure 6g,h). Therefore, even if any tiny fractures occur at the stress-concentrated edge of vertically synthesized nanowires, the bond between the electrode and the nanowires in the most area is robust. Thus, the fractures at the edge rarely affect the electrical connection between nanowires and electrode. The stress applied at the nanowires is a more suitable parameter to evaluate the mechanical strength of the device. As shown in Table S1b, the maximum stress applied to horizontally integrated nanowire samples was 5.180 and 5.175 GPa with 2 and 5 μm length under 2% tensile stress, respectively. The maximum stress applied to 5 μm long, vertically synthesized nanowire was 0.215 GPa, which is only 4.2% of that applied to the horizontally integrated nanowire sample. Moreover, even if the substrate was stretched by 2% because of the bending, the maximum strain on the 5 μm long nanowire sample was only 0.114% because long nanowire that was vertically oriented, could spread out and diminish the tensile stress. Under compressive loading, compressive stresses were applied to the samples and the magnitudes of compressive stresses were the same as those under tensile loading (Figure S7a−d). In order to visually observe the mechanical robustness of the nanowires under bending or tensile loading conditions, the devices were stretched up to a tensile strain of 7.5% and recovered. As shown in Figure 7, the nanowires were gradually bent by

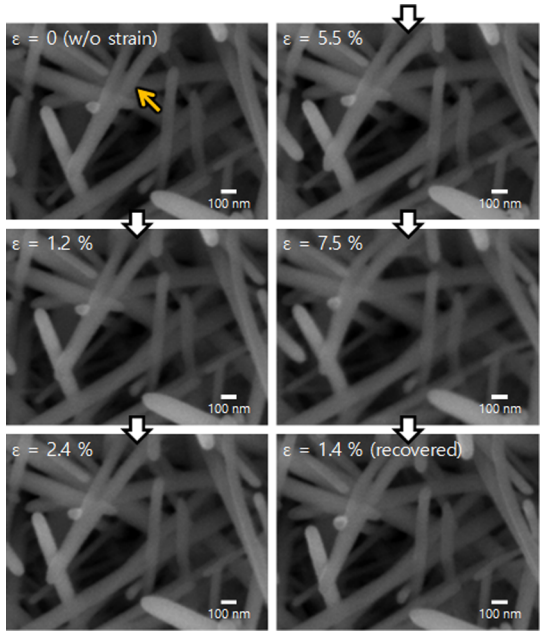

Figure 7. SEM images during tensile condition with various strains [ε = 0 (w/o strain), ε = 1.2%, ε = 2.4%, ε = 5.5%, ε = 7.5%, and ε = 1.4% (recovered, w/o tensile force)].

increasing strain. After releasing the device to a zero tensile force, the substrate had a permanent deformation of 1.4%, but the nanowires were not deformed. Even though the substrate was stretched by 7.5%, the bending of vertically grown nanowires was much smaller. This corresponds to the numerical simulation results and verifies the mechanical robustness of vertically grown nanowires under bending condition. In summary, vertically grown nanowires provide longer junction length and bending stress is decreased throughout the nanowires. Therefore, the vertically oriented nanostructure allows the avoidance of the fracture and significant change of electrical characteristics of the nanowire network. Our flexible H_2S gas sensors showed not only good mechanical robustness under mechanical stress but also comparable H_2S gas sensing performance to other rigid type gas sensors (Table S3).

CONCLUSIONS

In summary, Pd nanoparticle-decorated ZnO/ZnS core−shell nanowires were synthesized by using sequential combination of localized hydrothermal synthesis, liquid phase deposition process, and surface sulfurization. This method enables facile synthesis and direct integration of sensing nanomaterials within 100^2 μm^2 area as well as their surface functionalization with the Pd catalyst. Moreover, the nanomaterials were synthesized on a flexible polymer substrate due to the reaction at low temperature (<95 °C) in a mild precursor solution. The devices were treated with H_2S gas for stable sensing characteristics and showed outstanding H_2S gas sensing performance because of the catalytic effect of Pd nanoparticles [$(G_{gas} - G_{air})/G_{air} \times 100\%$ = 4491% to 10 ppm] as well as stable sensing performance under both positive (ρ = 9 mm) and negative (ρ = −5 mm) bending conditions because of

DOI: 10.1021/acsami.9b06951
ACS Appl. Mater. Interfaces 2019, 11, 24298−24307

robust bonding between the sensing material and electrodes and long bending path. This method enables the facile fabrication of flexible, highly sensitive, and mechanically robust gas sensors for toxic gases via an eco-friendly manufacturing process. The flexible gas sensor developed in this work can be widely used for practical applications in wearable sensing and internet of things systems because of their high performance, simple fabrication, small size, and mechanical flexibility.

■ ASSOCIATED CONTENT

Supporting Information

The Supporting Information is available free of charge on the ACS Publications website at DOI: 10.1021/acsami.9b06951.

Fabrication process of the flexible microheater device; estimation of temperature of the microheater; TEM analysis of sulfurized ZnO/ZnS core−shell nanowires; synthesis of uniform ZnO nanowires by in situ current measurement; EDS data after palladium (Pd) decoration; numerical simulation of ZnO nanowire devices under positive bending; numerical simulation of ZnO nanowire devices under negative bending; and comparison of performance with state-of-the-art research studies (PDF)

■ AUTHOR INFORMATION

Corresponding Author

*E-mail: inkyu@kaist.ac.kr.

ORCID

Daejong Yang: 0000-0002-8774-5843

Inkyu Park: 0000-0001-5761-7739

Author Contributions

D.Y. and I.C. contributed equally. The manuscript was written through contributions of all authors. All authors have given approval to the final version of the manuscript.

Notes

The authors declare no competing financial interest.

■ ACKNOWLEDGMENTS

This work was supported by (1) Multi-Ministry Collaborative R&D Program (Development of Techniques for Identification and Analysis of Gas Molecules to Protect Against Toxic Substances) through the National Research Foundation of Korea (NRF) funded by KNPA, MSIT, MOTIE, ME, NFA (NRF-2017M3D9A1073858) and (2) "Development of Management Technology for HNS Accident (D11502815H480000140 2015034016)" funded by the Ministry of Oceans and Fisheries, South Korea.

■ REFERENCES

(1) Bai, S.; Sun, C.; Wan, P.; Wang, C.; Luo, R.; Li, Y.; Liu, J.; Sun, X. Transparent Conducting Films of Hierarchically Nanostructured Polyaniline Networks on Flexible Substrates for High-Performance Gas Sensors. *Small* **2015**, *11*, 306−310.

(2) Choi, H.; Choi, J. S.; Kim, J.-S.; Choe, J.-H.; Chung, K. H.; Shin, J.-W.; Kim, J. T.; Youn, D.-H.; Kim, K.-C.; Lee, J.-I.; Choi, S.-Y.; Kim, P.; Choi, C.-G.; Yu, Y.-J. Flexible and Transparent Gas Molecule Sensor Integrated with Sensing and Heating Graphene Layers. *Small* **2014**, *10*, 3685−3691.

(3) Duy, L. T.; Trung, T. Q.; Dang, V. Q.; Hwang, B.-U.; Siddiqui, S.; Son, I.-Y.; Yoon, S. K.; Chung, D. J.; Lee, N.-E. Flexible Transparent Reduced Graphene Oxide Sensor Coupled with Organic Dye Molecules for Rapid Dual-Mode Ammonia Gas Detection. *Adv. Funct. Mater.* **2016**, *26*, 4329−4338.

(4) Fang, Y.; Akbari, M.; Sydänheimo, L.; Ukkonen, L.; Tentzeris, M. M. Sensitivity Enhancement of Flexible Gas Sensors via Conversion of Inkjet-Printed Silver Electrodes into Porous Gold Counterparts. *Sci. Rep.* **2017**, *7*, 8988.

(5) Khim, D.; Ryu, G.-S.; Park, W.-T.; Kim, H.; Lee, M.; Noh, Y.-Y. Precisely Controlled Ultrathin Conjugated Polymer Films for Large Area Transparent Transistors and Highly Sensitive Chemical Sensors. *Adv. Mater.* **2016**, *28*, 2752−2759.

(6) Kim, Y. H.; Kim, S. J.; Kim, Y.-J.; Shim, Y.-S.; Kim, S. Y.; Hong, B. H.; Jang, H. W. Self-Activated Transparent All-Graphene Gas Sensor with Endurance to Humidity and Mechanical Bending. *ACS Nano* **2015**, *9*, 10453−10460.

(7) Wan, P.; Wen, X.; Sun, C.; Chandran, B. K.; Zhang, H.; Sun, X.; Chen, X. Flexible Transparent Films Based on Nanocomposite Networks of Polyaniline and Carbon Nanotubes for High-Performance Gas Sensing. *Small* **2015**, *11*, 5409−5415.

(8) Yun, Y. J.; Hong, W. G.; Choi, N. J.; Kim, B. H.; Jun, Y.; Lee, H. K. Ultrasensitive and Highly Selective Graphene-Based Single Yarn for Use in Wearable Gas Sensor. *Sci. Rep.* **2015**, *5*, 10904.

(9) Yang, W.; Gan, L.; Li, H.; Zhai, T. Two-Dimensional Layered Nanomaterials for Gas-Sensing Applications. *Inorg. Chem. Front.* **2016**, *3*, 433−451.

(10) Athauda, T. J.; Hari, P.; Ozer, R. R. Tuning Physical and Optical Properties of ZnO Nanowire Arrays Grown on Cotton Fibers. *ACS Appl. Mater. Interfaces* **2013**, *5*, 6237−6246.

(11) Hwang, I.-S.; Kim, S.-J.; Choi, J.-K.; Jung, J.-J.; Yoo, D. J.; Dong, K.-Y.; Ju, B.-K.; Lee, J.-H. Large-Scale Fabrication of Highly Sensitive SnO_2 Nanowire Network Gas Sensors by Single Step Vapor Phase Growth. *Sens. Actuators, B* **2012**, *165*, 97−103.

(12) Liu, J.; Wu, W.; Bai, S.; Qin, Y. Synthesis of High Crystallinity ZnO Nanowire Array on Polymer Substrate and Flexible Fiber-Based Sensor. *ACS Appl. Mater. Interfaces* **2011**, *3*, 4197−4200.

(13) Steinhauer, S.; Brunet, E.; Maier, T.; Mutinati, G. C.; Köck, A. Suspended CuO Nanowires for ppb Level H_2S Sensing in Dry and Humid Atmosphere. *Sens. Actuators, B* **2013**, *186*, 550−556.

(14) Van Hieu, N.; Van Vuong, H.; Van Duy, N.; Hoa, N. D. A Morphological Control of Tungsten Oxide Nanowires by Thermal Evaporation Method for Sub-ppm NO_2 Gas Sensor Application. *Sens. Actuators, B* **2012**, *171−172*, 760−768.

(15) Wang, C.; Yin, L.; Zhang, L.; Xiang, D.; Gao, R. Metal Oxide Gas Sensors: Sensitivity and Influencing Factors. *Sensors* **2010**, *10*, 2088−2106.

(16) Yang, J.; Hidajat, K.; Kawi, S. Synthesis Of Nano-SnO_2/SBA-15 Composite as a Highly Sensitive Semiconductor Oxide Gas Sensor. *Mater. Lett.* **2008**, *62*, 1441−1443.

(17) Yu, H.; Li, J.; Loomis, R. A.; Wang, L.-W.; Buhro, W. E. Two- versus three-dimensional quantum confinement in indium phosphide wires and dots. *Nat. Mater.* **2003**, *2*, 517.

(18) Son, J. Y.; Lim, S. J.; Cho, J. H.; Seong, W. K.; Kim, H. Synthesis of Horizontally Aligned ZnO Nanowires Localized at Terrace Edges and Application for High Sensitivity Gas Sensor. *Appl. Phys. Lett.* **2008**, *93*, 053109.

(19) Ahn, J.-H.; Yun, J.; Choi, Y.-K.; Park, I. Palladium Nanoparticle Decorated Silicon Nanowire Field-Effect Transistor with Side-Gates for Hydrogen Gas Detection. *Appl. Phys. Lett.* **2014**, *104*, 013508.

(20) Chen, Z. H.; Jie, J. S.; Luo, L. B.; Wang, H.; Lee, C. S.; Lee, S. T. Applications of Silicon Nanowires Functionalized with Palladium Nanoparticles in Hydrogen Sensors. *Nanotechnology* **2007**, *18*, 345502.

(21) da Silva, L. F.; Catto, A. C.; Avansi, W.; Cavalcante, L. S.; Andrés, J.; Aguir, K.; Mastelaro, V. R.; Longo, E. A Novel Ozone Gas Sensor Based on One-Dimensional (1D) α-Ag_2WO_4 Nanostructures. *Nanoscale* **2014**, *6*, 4058−4062.

(22) Kim, N.-H.; Choi, S.-J.; Yang, D.-J.; Bae, J.; Park, J.; Kim, I.-D. Highly Sensitive and Selective Hydrogen Sulfide and Toluene Sensors using Pd Functionalized WO_3 Nanofibers for Potential Diagnosis of Halitosis and Lung Cancer. *Sens. Actuators, B* **2014**, *193*, 574−581.

(23) Kolmakov, A.; Moskovits, M. Chemical Sensing and Catalysis by One-Dimensional Metal-Oxide Nanostructures. *Annu. Rev. Mater. Res.* **2004**, *34*, 151−180.
(24) Tien, L. C.; Wang, H. T.; Kang, B. S.; Ren, F.; Sadik, P. W.; Norton, D. P.; Pearton, S. J.; Lin, J. Room-Temperature Hydrogen-Selective Sensing using Single Pt-Coated ZnO Nanowires at Microwatt Power Levels. *Electrochem. Solid-State Lett.* **2005**, *8*, G230−G232.
(25) Lupan, O.; Postica, V.; Adelung, R.; Labat, F.; Ciofini, I.; Schürmann, U.; Kienle, L.; Chow, L.; Viana, B.; Pauporté, T. Functionalized Pd/ZnO Nanowires for Nanosensors. *Phys. Status Solidi* **2018**, *12*, 1700321.
(26) Lupan, O.; Postica, V.; Labat, F.; Ciofini, I.; Pauporté, T.; Adelung, R. Ultra-Sensitive and Selective Hydrogen Nanosensor with Fast Response at Room Temperature based on a Single Pd/Zno Nanowire. *Sens. Actuators, B* **2018**, *254*, 1259−1270.
(27) Chávez, F.; Pérez-Sánchez, G. F.; Goiz, O.; Zaca-Morán, P.; Peña-Sierra, R.; Morales-Acevedo, A.; Felipe, C.; Soledad-Priego, M. Sensing Performance of Palladium-Functionalized WO_3 Nanowires by a Drop-Casting Method. *Appl. Surf. Sci.* **2013**, *275*, 28−35.
(28) Fiorido, T.; Bendahan, M.; Aguir, K.; Bernardini, S.; Martini, C.; Brisset, H.; Fages, F.; Videlot-AckermannC, C.; Ackermann, J. All solution processed flexible ammonia gas and light sensors based on α,ω-hexyl-distyrylbithiophene films. *Sens. Actuators, B* **2010**, *151*, 77−82.
(29) Kang, K.; Yang, D.; Park, J.; Kim, S.; Cho, I.; Yang, H.-H.; Cho, M.; Mousavi, S.; Choi, K. H.; Park, I. Micropatterning of Metal Oxide Nanofibers by Electrohydrodynamic (EHD) Printing towards Highly Integrated and Multiplexed Gas Sensor Applications. *Sens. Actuators, B* **2017**, *250*, 574−583.
(30) Kim, J.-W.; Porte, Y.; Ko, K. Y.; Kim, H.; Myoung, J.-M. Micropatternable Double-Faced ZnO Nanoflowers for Flexible Gas Sensor. *ACS Appl. Mater. Interfaces* **2017**, *9*, 32876−32886.
(31) Uddin, A. S. M. I.; Yaqoob, U.; Chung, G.-S. Improving the Working Efficiency of a Triboelectric Nanogenerator by the Semimetallic PEDOT:PSS Hole Transport Layer and Its Application in Self-Powered Active Acetylene Gas Sensing. *ACS Appl. Mater. Interfaces* **2016**, *8*, 30079−30089.
(32) Lupan, O.; Pauporté, T. Hydrothermal Treatment for the Marked Structural and Optical Quality Improvement of ZnO Nanowire Arrays Deposited on Lightweight Flexible Substrates. *J. Cryst. Growth* **2010**, *312*, 2454−2458.
(33) Xu, S.; Weintraub, B.; Wang, Z. L. Zinc Oxide Nanowire Arrays on Flexible Substrates: Wet Chemical Growth and Applications in Energy Conversion. *Semiconductor Nanomaterials for Flexible Technologies*; Elsevier, 2010; pp 197−226.
(34) Yoon, J.; Sun, Y.; Rogers, J. A. Flexible Solar Cells Made of Nanowires/Microwires. *Semiconductor Nanomaterials for Flexible Technologies*; Elsevier, 2010; pp 159−196.
(35) Hsu, N.-F.; Chang, M.; Lin, C.-H. Synthesis of ZnO Thin Films and Their Application as Humidity Sensors. *Microsyst. Technol.* **2013**, *19*, 1737−1743.
(36) Yang, D.; Kim, D.; Ko, S. H.; Pisano, A. P.; Li, Z.; Park, I. Focused Energy Field Method for the Localized Synthesis and Direct Integration of 1D Nanomaterials on Microelectronic Devices. *Adv. Mater.* **2015**, *27*, 1207−1215.
(37) Greene, L. E.; Law, M.; Tan, D. H.; Montano, M.; Goldberger, J.; Somorjai, G.; Yang, P. General Route To Vertical Zno Nanowire Arrays Using Textured ZnO Seeds. *Nano Lett.* **2005**, *5*, 1231−1236.
(38) Yang, D.; Fuadi, M. K.; Kang, K.; Kim, D.; Li, Z.; Park, I. Multiplexed Gas Sensor Based on Heterogeneous Metal Oxide Nanomaterial Array Enabled by Localized Liquid-Phase Reaction. *ACS Appl. Mater. Interfaces* **2015**, *7*, 10152−10161.
(39) Yang, D.; Kang, K.; Kim, D.; Li, Z.; Park, I. Fabrication of Heterogeneous Nanomaterial Array by Programmable Heating and Chemical Supply within Microfluidic Platform towards Multiplexed Gas Sensing Application. *Sci. Rep.* **2015**, *5*, 8149.
(40) Cho, I.; Kang, K.; Yang, D.; Yun, J.; Park, I. Localized Liquid-Phase Synthesis of Porous SnO_2 Nanotubes on Mems Platform for Low-Power, High Performance Gas Sensors. *ACS Appl. Mater. Interfaces* **2017**, *9*, 27111−27119.
(41) Choi, B.-S.; Lee, Y. W.; Kang, S. W.; Hong, J. W.; Kim, J.; Park, I.; Han, S. W. Multimetallic Alloy Nanotubes with Nanoporous Framework. *ACS Nano* **2012**, *6*, 5659−5667.
(42) Lee, Y. W.; Lim, M. A.; Kang, S. W.; Park, I.; Han, S. W. Facile Synthesis of Noble Metal Nanotubes by Using ZnO Nanowires as Sacrificial Scaffolds and Their Electrocatalytic Properties. *Chem. Commun.* **2011**, *47*, 6299−6301.
(43) Lim, M. A.; Kim, D. H.; Park, C.-O.; Lee, Y. W.; Han, S. W.; Li, Z.; Williams, R. S.; Park, I. A New Route toward Ultrasensitive, Flexible Chemical Sensors: Metal Nanotubes by Wet-Chemical Synthesis along Sacrificial Nanowire Templates. *ACS Nano* **2011**, *6*, 598−608.
(44) Chen, H.; Wu, X.; Gong, L.; Ye, C.; Qu, F.; Shen, G. Hydrothermally Grown ZnO Micro/Nanotube Arrays and Their Properties. *Nanoscale Res. Lett.* **2010**, *5*, 570.
(45) Barsan, N.; Koziej, D.; Weimar, U. Metal Oxide-Based Gas Sensor Research: How To? *Sens. Actuators, B* **2007**, *121*, 18−35.
(46) Eranna, G.; Joshi, B. C.; Runthala, D. P.; Gupta, R. P. Oxide Materials for Development of Integrated Gas Sensors-A Comprehensive Review. *Crit. Rev. Solid State Mater. Sci.* **2004**, *29*, 111−188.
(47) Kim, S.-J.; Hwang, I.-S.; Kang, Y. C.; Lee, J.-H. Design of Selective Gas Sensors Using Additive-Loaded In_2O_3 Hollow Spheres Prepared by Combinatorial Hydrothermal Reactions. *Sensors* **2011**, *11*, 10603−10614.
(48) Williams, D. E. Semiconducting Oxides as Gas-Sensitive Resistors. *Sens. Actuators, B* **1999**, *57*, 1−16.
(49) Kim, J.; Yong, K. Mechanism Study of ZnO Nanorod-Bundle Sensors for H_2S Gas Sensing. *J. Phys. Chem. C* **2011**, *115*, 7218−7224.
(50) Bai, Z.; Xie, C.; Hu, M.; Zhang, S.; Zeng, D. Effect of Humidity on the Gas Sensing Property of The Tetrapod-Shaped ZnO Nanopowder Sensor. *Mater. Sci. Eng., B* **2008**, *149*, 12−17.
(51) Qi, G.; Zhang, L.; Yuan, Z. Improved H_2S Gas Sensing Properties of ZnO Nanorods Decorated by a Several nm ZnS Thin Layer. *Phys. Chem. Chem. Phys.* **2014**, *16*, 13434−13439.
(52) Occupational Safety and Health Administration (OSHA). *Toxic and Hazardous Substances 1915.1000*; Occupational Safety and Health Administration: Washington, D.C., USA, 2017.
(53) Han, J.; Liu, Z.; Zheng, X.; Guo, K.; Zhang, X.; Hong, T.; Wang, B.; Liu, J. Trilaminar ZnO/ZnS/Sb_2S_3 Nanotube Arrays for Efficient Inorganic−Organic Hybrid Solar Cells. *RSC Adv.* **2014**, *4*, 23807−23814.
(54) Li, P.; Deng, S.; Zhang, L.; Liu, G.; Yu, J. Native Point Defects in ZnS: First-Principles Studies based on LDA, LDA+ U and an Extrapolation Scheme. *Chem. Phys. Lett.* **2012**, *531*, 75−79.
(55) Chen, Z.-G.; Zou, J.; Liu, G.; Lu, H. F.; Li, F.; Lu, G. Q.; Cheng, H. M. Silicon-Induced Oriented ZnS Nanobelts for Hydrogen Sensitivity. *Nanotechnology* **2008**, *19*, 055710.
(56) Zhang, W.; Wang, S.; Wang, Y.; Zhu, Z.; Gao, X.; Yang, J.; Zhang, H. x. ZnO@ZnS core/shell microrods with enhanced gas sensing properties. *RSC Adv.* **2015**, *5*, 2620−2629.
(57) Sung, Y.-M.; Noh, K.; Kwak, W.-C.; Kim, T. G. Enhanced Glucose Detection Using Enzyme-Immobilized ZnO/ZnS Core/Sheath Nanowires. *Sens. Actuators, B* **2012**, *161*, 453−459.
(58) Bui, C. T.; Xie, R.; Zheng, M.; Zhang, Q.; Sow, C. H.; Li, B.; Thong, J. T. L. Diameter-Dependent Thermal Transport in Individual ZnO Nanowires and its Correlation with Surface Coating and Defects. *Small* **2012**, *8*, 738−745.
(59) Rule, D. L.; Smith, D. R.; Sparks, L. L. Thermal Conductivity of Polypyromellitimide Film with Alumina Filler Particles from 4.2 to 300 K. *Cryogenics* **1996**, *36*, 283−290.
(60) Zhang, D.; Jin, C.; Tian, H.; Xiong, Y.; Zhang, H.; Qiao, P.; Fan, J.; Zhang, Z.; Li, Z. Y.; Li, J. An In Situ TEM Study of the Surface Oxidation of Palladium Nanocrystals Assisted by Electron Irradiation. *Nanoscale* **2017**, *9*, 6327−6333.
(61) Teichner, S. J. Recent Studies in Hydrogen and Oxygen Spillover and Their Impact on Catalysis. *Appl. Catal.* **1990**, *62*, 1−10.

DOI: 10.1021/acsami.9b06951
ACS Appl. Mater. Interfaces 2019, 11, 24298−24307

(62) Ghiotti, G.; Chiorino, A.; Boccuzzi, F. Infrared Study of Surface Chemistry and Electronic Effects of Different Atmospheres on SnO_2. *Sens. Actuators* **1989**, *19*, 151−157.
(63) Lupan, O.; Postica, V.; Hoppe, M.; Wolff, N.; Polonskyi, O.; Pauporté, T.; Viana, B.; Majérus, O.; Kienle, L.; Faupel, F.; Adelung, R. PdO/PdO_2 functionalized ZnO : Pd films for lower operating temperature H_2 gas sensing. *Nanoscale* **2018**, *10*, 14107−14127.
(64) Zhang, M.; Ning, T.; Zhang, S.; Li, Z.; Cao, Q.; Yuan, Z. Comparison of Pt and Pd Modified TiO_2 Gas Sensors. *Mater. Sci.* **2014**, *20*, 375−380.
(65) Wen, B.; Sader, J. E.; Boland, J. J. Mechanical Properties of ZnO Nanowires. *Phys. Rev. Lett.* **2008**, *101*, 175502.

DOI: 10.1021/acsami.9b06951
ACS Appl. Mater. Interfaces 2019, 11, 24298−24307